Solution Structure of the Complex between the B-Subunit Homopentamer of Verotoxin VT-1 from *Escherichia coli* and the Trisaccharide Moiety of Globotriaosylceramide†

H. Shimizu,‡ R. A. Field,‡ S. W. Homans,*,‡ and A. Donohue-Rolfe§

Centre for Biomolecular Sciences, University of St. Andrews, St. Andrews, FIFE, KY16 9ST, U.K., and Department of Comparative Medicine, Tufts University School of Veterinary Medicine, 200 Westboro Road, N. Grafton, Massachusetts 01536

Received April 27, 1998; Revised Manuscript Received June 5, 1998

ABSTRACT: We report the solution structure of the carbohydrate-binding B subunit of verotoxin VT-1 (VTB) from enterohemorrhagic *Escherichia coli* in association with the trisaccharide Galα1−4Galβ1−4Glcβ1-*O*-trimethylsilylethyl, determined by use of stable isotope-assisted NMR techniques. In contrast to the crystal structure of the complex which predicts three binding sites per monomer, only one of these sites is observed with substantial occupancy by the trisaccharide in solution.

The verotoxins are representative of the AB_5 class of bacterial toxins whose morphology comprises an enzymatic A subunit in which the toxic activity resides, associated with a B oligomer that binds to specific cell-surface carbohydrate receptors (*1*−*3*). This receptor is globotriaosylceramide (Gb_3; Galα1−4Galβ1−4Glc-Cer) in the case of verotoxin-1, and the inhibition of this interaction is the basis of a new proposed therapy (*4*). Both the crystal (*5*) and NMR (*6*) structures of the B subunit of verotoxin-1 (VTB)[1] from enterohemorrhagic *Escherichia coli* have been solved, but the solution structure of the complex between VTB and the carbohydrate receptor has not been reported. Here, we describe the solution structure of the complex between VTB and the trimethylsilylethyl derivative of the trisaccharide moiety of Gb_3 (Gb_3OSE, Galα1−4Galβ1−4Glcβ1-*O*-trimethylsilylethyl) determined by use of stable-isotope assisted high-resolution NMR methods with ^{13}C-enriched Gb_3OSE and effect a comparison with the recently determined crystal structure of the complex (*7*). The latter exhibits three binding sites for the glycan. The first, termed "site 1", is similar to the site predicted by Nyholm et al. (*8, 9*), and is characterized by a stacking interaction of Galβ with the side chain of Phe 30. The second site ("site 2") is topologically equivalent to the binding sites found in the other OB fold proteins and is similar to a second site predicted by Nyholm et al. The third site ("site 3") involves a stacking interaction of Galβ on the side chain of Trp 34.

MATERIALS AND METHODS

Uniformly ^{15}N-enriched VTB was expressed and purified as described (*6*). Uniformly ^{13}C-enriched Galα1−4Galβ1−4Glc was prepared by chemical synthesis using uniformly ^{13}C-enriched D-glucose as starting material. Full details of this synthesis will be described elsewhere. Two-dimensional ^{13}C-^{1}H-HSQC (*10*) and three-dimensional NOESY-HSQC experiments were recorded at 500 MHz with a Varian Unity plus spectrometer using a sample containing 1.3 mg of Galα1−4Galβ1−4Glcβ1-OSE uniformly ^{13}C-enriched in the glycan moiety and 10 mg (1:1 complex) or 1 mg of purified VTB (1:10 complex) in 0.7 mL of 100 mM phosphate buffer, pH 7.0, prepared in 99.96% D_2O. The probe temperature was 300 K in all experiments. A total of 128 × 512 and 128 × 32 × 512 complex points were acquired in the F1, F2 and F1, F2, F3 dimensions of two- and three-dimensional spectra, respectively, with proton spectral widths of 1050 Hz (3825 Hz in NOESY-HSQC spectra of the 1:1 complex) and carbon spectral widths of 2900 Hz. Prior to two- and three-dimensional Fourier transformation, time-domain data were apodized with cosine-bell weighting functions in F1,-F2 (HSQC spectra) or with cosine bell weighting functions in F1,F2 and a 10 Hz line-broadening function in F3 (NOESY-HSQC spectra). ^{15}N-^{1}H HSQC experiments were recorded using a sample containing 3 mg of uniformly ^{15}N-enriched VTB and 1.2 mg of Galα1−4Galβ1−4Glcβ1-OSE in 0.7 mL of phosphate buffer, pH 7.0, prepared in 95% H_2O/5% D_2O. Solvent suppression was achieved by use of the WATERGATE technique (*11*).

Experimental TRNOE intensities were measured directly as volume integrals from two-dimensional F1/F3 planes derived from three-dimensional NOESY-HSQC spectra, and integrals were summed for each plane that contained a contribution from the relevant cross-peak to give the three-dimensional volume integral. Transferred NOE simulations were computed with the in-house written software package MDNOE2. This package incorporates a full-relaxation matrix analysis of TRNOEs (*12*) and includes a formalism for computation of the relaxation matrix which accounts for internal motions which are fast with respect to the rotational tumbling time (*13*). Simulations utilized the following parameters. Rotational correlation time of the ligand (τ_{cL}) = 0.12 ns; rotational correlation time of the complex (τ_{cR})

† This work was suppported by BBSRC Grant 49/SBD07527.

* Author to whom correspondence should be addressed.

‡ University of St. Andrews.

§ Tufts University School of Veterinary Medicine.

[1] Abbreviations: Gb_3OSE, Galα1−4Galβ1−4Glcβ1-*O*-trimethylsilylethyl; HSQC, heteronuclear single-quantum correlation; NOESY-HSQC, three-dimensional nuclear Overhauser effect-heteronuclear single-quantum correlation spectroscopy; NOE, nuclear Overhauser effect; TRNOE, transferred nuclear Overhauser effect; VTB, Verotoxin B subunit.

S0006-2960(98)00946-5 CCC: $15.00
Published on Web 07/16/1998

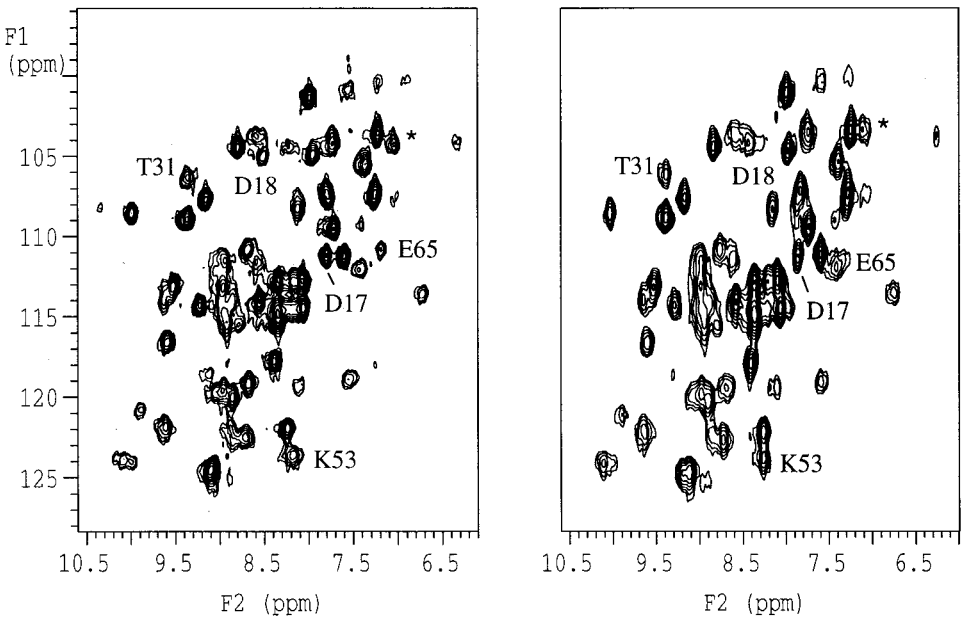

FIGURE 1: ^{15}N-^{1}H-HSQC spectra of uniformly ^{15}N-enriched VTB in the absence (left panel) and presence (1:1, w/w) of Gb_3OSE ligand (right panel). Shift perturbations arising from binding of ligand are labeled using the conventional single-letter amino acid code. An unassigned resonance that shifts on ligand binding is marked with an asterisk.

Table 1: Shifts of Backbone HN Resonances of VTB That Are Observable within Experimental Error upon Binding of Gb_3OSE Ligand (1:1 mol/mol)

HN resonance[a]	shift (Hz)[b]	HN resonance[a]	shift (Hz)[b]
Asp 17	+21.1	Lys 53	+28.0
Asp 18	−49.2	Glu 65	+19.2
Thr 31	−7.1	unassigned	+24.6

[a] Resonances not listed experience no measurable shift within experimental error. [b] The digital resolution in the HN dimension was ±1.8 Hz. Total estimated error including error in peak picking is ±6 Hz.

= 18 ns; reduced rate constant (k) = 1000 s^{-1}; dissociation constant (K_d) = 2 mM; concentration of VTB ([R]) = 1.9 mM (1:1 complex) or 0.19 mM (1:10 complex); concentration of Gb_3OSE ([L]) = 1.9 mM; mixing time (τ_m) = 0.1 s or 0.2 s in NOESY-HSQC spectra of the 1:10 complex. All parameters were known except the value of k. This was varied iteratively to obtain the best fit between theoretical and experimental volume integrals of diagonal vs cross-peak intensities for an internal reference distance. In practice, the theoretical TRNOE intensities were not very sensitive to this parameter.

RESULTS AND DISCUSSION

In an effort to determine the location of the binding site(s) for the glycan in solution, ^{15}N-^{1}H heteronuclear single-quantum correlation (HSQC) experiments (*10*) were performed on uniformly (^{15}N) enriched VTB in both the absence and the presence of Gb_3OSE ligand. By use of ^{15}N and ^{1}H resonance assignments of VTB determined previously (*6*), observed resonance shifts on binding (Figure 1 and Table 1) were assignable to Asp 17, Asp 18, Thr 31, Lys 53, and Glu 65. All of these residues are sufficiently proximal to sites 1 and 2 in the crystal structure to suggest that shift perturbations might occur when either site is occupied. One further resonance shift was also observed, which corresponds with one of the seven unassigned HN resonances in the protein (Val 5, Tyr 14, Asn 15, Asp 16, Ser 38, Asn 55, Asn 59). However, it is notable that there is no measurable shift perturbation of Trp 34 NH. The side chain of this residue, which forms part of site 3 in the crystal structure, undergoes a significant conformational change on binding ligand, giving rise to a predicted shift (*14*, *15*) of ~110 Hz upfield assuming 100% occupancy at that site. The absence of any shift perturbations on this residue or indeed any other residues in the vicinity of Trp 34, therefore, suggests that site 3 is essentially unoccupied in solution.

To establish whether either or both of sites 1 and 2 are occupied in solution, an attempt was made to observe intermolecular ligand−protein NOEs. In general, such NOEs are observable with difficulty (*16*) or not at all in systems involving chemical exchange that is fast on the NMR time scale, usually as a result of the tendency to utilize high ligand:protein ratios (>5:1) in order to observe intraligand transferred NOEs (TRNOEs) without interference from protein resonances. Under these conditions, ligand−protein TRNOEs are weak due to the low bound fraction of ligand. In the present study, we utilized uniformly enriched trisaccharide ligand prepared by chemical synthesis, which enabled a much lower ligand−protein ratio (1:1) to be employed in isotope-edited HSQC-NOESY experiments. In view of the severe resonance overlap and line-broadening of resonances in the ^{1}H NMR spectrum of the complex, a three-dimensional HSQC-NOESY experiment was utilized, thus enabling spectral editing in the second (^{13}C) dimension. Sections from typical F1/F3 (^{1}H/^{1}H) planes from this experiment are illustrated in Figure 2, from which it is seen that TRNOEs are detectable from Galβ H-1 and H-3 and Glcβ H-4 to the methyl group of Ala 56. This assignment to Ala 56 is unambiguous since the only other methyl group that resonates in a similar position (0.04 ppm lower in resonance frequency) is that of Thr 46, which is not involved in any of the binding sites in the crystal structure and indeed is located on the opposite face of the pentamer. These observations immediately suggest substantial occupancy of site 2 (Figure 3), and indeed the intensities of the experimental ligand−

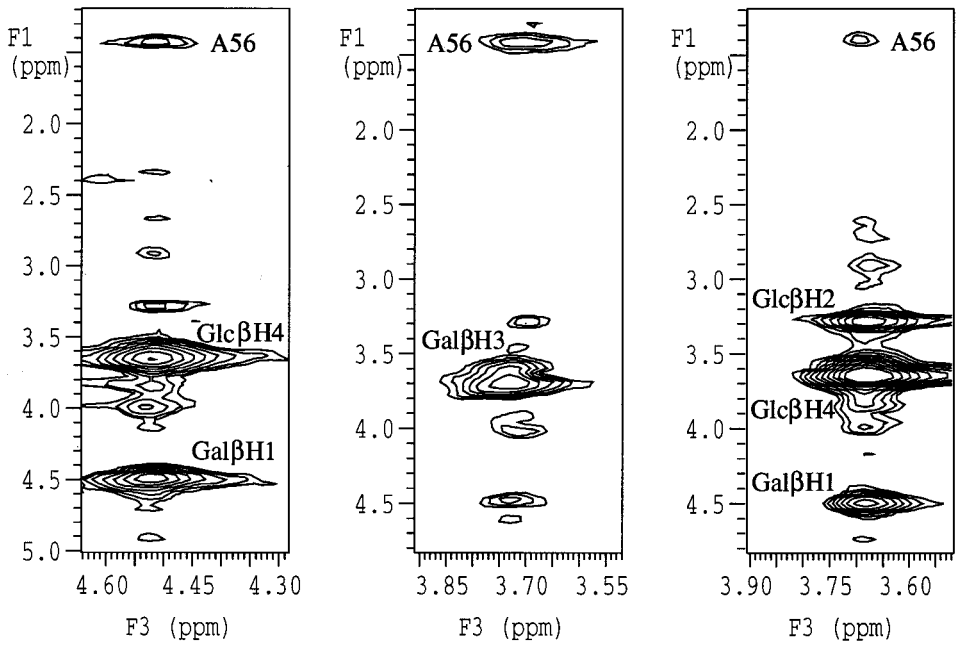

FIGURE 2: Two-dimensional F1/F3 planes derived from the three-dimensional NOESY-HSQC spectrum (τ_m = 0.1 s) of VTB in complex with uniformly ^{13}C-enriched Gb_3OSE (1:1, w/w). Planes correspond with the ^{13}C resonance frequencies of Galβ C-1 (left panel, F3 = 104.1 ppm), Galβ C-3 (middle panel, F3 = 73.0 ppm), and Glcβ C-4 (right panel, F3 = 79.5 ppm). Intermolecular TRNOEs to Ala 56 are labeled.

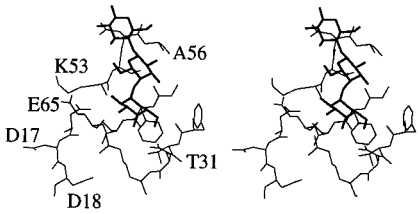

FIGURE 3: Stereoview of site 2 derived from the crystal structure of the VTB−Gb_3 complex (*7*), highlighting the residues whose N−H resonances experience shifts on ligand binding (Figure 1), together with Ala 56, whose methyl group exhibits NOE connectivities to ligand protons (see text for details).

protein TRNOEs are in good agreement with predicted values computed with the relevant experimental conditions, assuming that only site 2 is occupied (Table 2). Given the inaccuracies both in volume integration of the relevant TRNOEs, together with uncertainties in the theoretical values at the available resolution of the crystal structure (*7*), the TRNOE data cannot alone be used to rule out occupancy at site 1. However, substantial TRNOEs are predicted at this site from the crystal structure from Galβ H-4 to Phe 30 Hδ2 and Hϵ2 (Table 2). Despite intensive effort, no such TRNOEs were observable in the 3D HSQC-NOESY spectrum. Taking into account the finite signal-to-noise ratio in the latter, these data taken together, therefore, suggest that the occupancy at site 1 is at most 15% relative to site 2 in solution. The absence of the large ligand−protein TRNOEs predicted for site 3 (Table 2) provides further evidence that this site is essentially unoccupied in solution.

Given that the bound-state conformation of the ligand is essentially identical in sites 1 and 2 in the crystal structure, we sought to confirm whether this conformation was preserved in solution by use of TRNOE measurements identical to those described above but at a higher ligand:protein ratio (10:1) for optimal measurement of intraligand NOEs. It should be remarked that even in this case where the resonance line widths are much smaller than in the 1:1 complex, due to severe resonance overlap, it was still necessary to resort to three-dimensional NOESY-HSQC

Table 2: Experimental vs Predicted Ligand−Protein and Ligand−Ligand TRNOE Intensities Derived from 3D NOESY-HSQC Data on VTB in Association with Uniformly ^{13}C-Enriched Galα1−4Galβ1−4Glcβ1−OSE

connectivity	experimental TRNOE (%)	theoretical TRNOE (%)[a]
VTB: Gb_3OSE (1:1)		
site 2		
Galβ H-1−Galβ H-3/5	−12.9	−12.9[b]
Galβ H-1−Ala 56 CH_3	−1.3	−1.6
Galβ H-3−Ala 56 CH_3	−2.6	−3.5
Glcβ H-4−Ala 56 CH_3	−0.5	−0.5
site 1		
Galβ H-4−Phe 30 Hδ1	nd[c]	−0.7
Galβ H-4−Phe 30 Hδ2	nd	−2.9
Galβ H-4−Phe 30 Hϵ1	nd	−0.4
Galβ H-4−Phe 30 Hϵ2	nd	−1.4
Galβ H-4−Phe 30 Hζ	nd	−0.6
site 3		
Galβ H-3−Trp 34 Hϵ3	nd	−3.2
Galβ H-3−Trp 34 Hζ3	nd	−1.7
Galβ H-5−Trp 34 Hζ2	nd	−1.5
Galβ H-5−Trp 34 Hη2	nd	−1.3
Galα H-1−Trp 34 Hβ1	nd	−0.7
Galα H-1−Trp 34 Hβ2	nd	−0.9
VTB:Gb_3OSE (1:10)		
site 2		
Galα H-1−Galα H-2	−1.8	−1.8[b]
Galα H-1−Galβ H-4	−2.1	−2.2
Galα H-1−Galβ H-6	−2.7	−2.4
Galα H-1−Galβ H-6′	−2.5	−3.1

[a] Values calculated by use of a full relaxation-matrix simulation with the crystal coordinates of the ligand and binding site residues in site 2. Parameters used were as follows (see experimental section for further details): τ_{cL} = 0.12 ns; τ_{cR} = 18 ns; k = 1000 s^{-1}; K_d = 2 mM; [R] = 1.9 mM or 0.19 mM; [L] = 1.9 mM, τ_m = 0.1 s (0.2 s for the 1:10 complex). [b] Theoretical value used as reference for calibration of experimental values. [c] nd, not detectable.

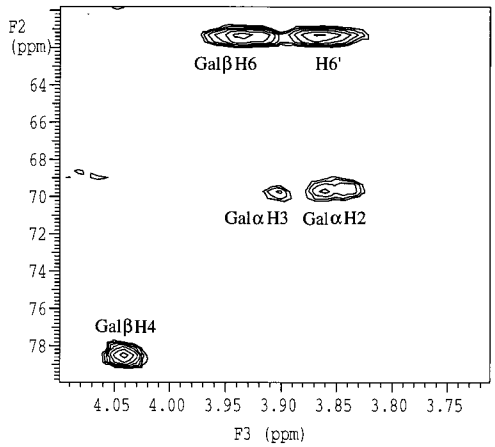

FIGURE 4: Two-dimensional F2/F3 derived from the three-dimensional NOESY-HSQC spectrum ($\tau_m = 0.2$ s) of VTB−Gb_3-OSE complex (1:10 w/w), at the F2 resonance frequency of Galα C-1 (101.1 ppm). Intramolecular TRNOEs are labeled.

Table 3: Comparison of Experimental ^{1}H Shift Perturbations in Gb_3OSE upon Addition of VTB (1:1), Compared with Theoretical Values Derived from Each of the Three Binding Sites Observed in the Crystal Structure of the Complex

	experimental shift (Hz)[b]		theoretical shift (Hz)[c]		
resonance[a]	i	ii	site 1	site 2	site 3
Galα					
H1	−8.7	−23.5	−228	−56	−6
H2	+16.0	+43.2	−237	+19	−46
H3	+11.0	+29.7	−99	−21	−28
H4	+26.3	+71.0	−43	−55	+103
H5	+2.6	+7.0	−70	−84	−11
Gal*β*					
H1	−3.1	−8.4	−143	+26	−211
H3	−7.1	−19.2	−93	+46	−587
H4	−4.5	−12.2	−593	−119	−1035
H5	−10.7	−28.9	−704	+116	−820

[a] Resonances not listed experience no measurable shift within experimental error. [b] Values listed are the measured shift (i) and the measured shift extrapolated to 100% bound ligand (ii) assuming K_d = 2 mM and protein and ligand concentrations of 1.9 mM. [c] Assuming 100% bound ligand in each site.

methods in order to obtain accurate volume integrals of TRNOE cross-peaks (Figure 4). The intensities of the resulting TRNOEs are in good agreement with those predicted from the crystal structure using a full-relaxation matrix calculation with the coordinates of site 2 (Table 2), suggesting that the bound-state conformation is preserved in solution.

The availability of uniformly ^{13}C-enriched Gb_3OSE enables shift perturbations in the ligand upon binding to VTB to be monitored accurately at high ligand−protein ratios by use of ^{13}C-^{1}H-HSQC experiments (not shown). Observed ^{1}H shifts resulting from addition of VTB to Gb_3OSE (1:1) are given in Table 3 and are compared with predicted theoretical shifts for each of the three binding sites in the crystal structure, assuming 100% occupancy of ligand at each site. It is notable that there is a very poor correlation between experimental and theoretical shift values, and indeed in some cases, the observed shift is the reverse of that predicted. The reason for these discrepancies lies primarily in the behavior of the pendant hydroxyl groups of residues involved in binding to VTB. In free solution, the majority of hydroxyl groups on carbohydrates exhibit freedom of motion about the respective C−O bond, as evidenced by the fact that the magnitude of the observed three-bond ^{1}H−^{1}H scalar coupling $^3J_{H-C-O-H}$ is similar to the average splitting assuming 360° rotation predicted from the relevant Karplus relation (*17*). The influence of the highly anisotropic hydroxyl oxygen atom on the shifts of nearby protons is therefore averaged by this motion. However, when hydroxyl groups partake in hydrogen bonding within a protein-binding site, the conformation about the C−O bond is essentially fixed, resulting in a very different shift perturbation on neighboring groups. Since no explicit theory exists for the magnitude of the shift perturbation arising from a hydroxyl group to our knowledge, these effects were therefore not considered in our theoretical predictions. However, it is possible to interpret these shifts in a qualitative sense. The overall influence of a hydroxyl group on the shifts of nearby nuclei is a tendency to shielding arising from the lone pairs located at the oxygen atom. In the bound state in site 2, the hydrogen-bonding interactions of the hydroxyl groups of, for example, Galα are such that the lone pairs at O-2, O-3, and O-4 are directed away from H-2, H-3, and H-4, respectively. The net effect will thus be deshielding relative to the average effect observed due to free rotation of the hydroxyl group in free solution, resulting in a downfield shift of H-2, H-3, and H-4 on binding. Finally, it is notable that very large upfield shifts are predicted for Gal*β* H-4 and H-5 in sites 1 and 3, yet only a modest shift is observed experimentally for each proton. The possibility that large upfield shifts arising from substantial occupancy of these sites is masked by large downfield shifts derived from hydrogen bonding involving neighboring hydroxyl groups is not tenable since only one such bond is formed from Gal*β*, namely from OH-3 in site 1. These observations therefore lend further support to the conclusion that sites 1 and 3 are not significantly occupied in solution.

CONCLUSIONS

On the basis of quantitative ligand−protein TRNOEs, together with qualitative chemical shift perturbations in both protein and ligand, it is proposed that only one of the three binding sites on VTB for the trisaccharide Galα1−4Gal*β*1−4Glc is substantially occupied with ligand in solution. The experimentally determined ligand−protein TRNOEs are in good agreement with theoretical values computed by use of a full-relaxation matrix simulation using the crystal coordinates of site 2. The lack of experimentally observable TRNOEs that are predicted to exist in site 1 from the crystal structure suggest that the occupancy of site 1 is <15% with respect to site 2. On the assumption that the effective dissociation constant (∼2 mM) for the VTB-Gb_3OSE interaction determined by titration microcalorimetry (*18*) derives primarily from site 1, these conclusions suggest that the dissociation constant at site 1 is greater than 6 mM. No evidence could be found for binding at site 3. Taken together, these observations are consistent with the crystallographic study, where the electron density for the ligand is strongest at site 2.

ACKNOWLEDGMENT

We thank Dr. Randy Read for providing coordinates of the crystal structure of the VTB−Gb_3 complex prior to release.

REFERENCES

1. Samuel, J. E., Perera, L. P., Ward, S., O'Brien, A. D., Ginsburg, V., and Krivan, H. C. (1990) *Infect. Immun. 58*, 611−618.
2. Waddell, T., Head, S., Petric, M., Cohen, A., and Lingwood, C. (1988) *Biochem. Biophys. Res. Commun. 152*, 674−679.
3. Lindberg, A. A., Brown, J. E., Stromberg, N., Westlingryd, M., Schultz, J. E., and Karlsson, K. A. (1987) *J. Biol. Chem. 262*, 1779−1785.
4. Armstrong, G. D., Rowe, P. C., Goodyer, P., Orrbine, E., Klassen, T. P., Wells, G., Mackenzie, A., Lior, H., Blanchard, C., Auclair, F., Thompson, B., Rafter, D. J., and McLaine, P. N. (1995) *J. Infect. Dis. 171*, 1042−1045.
5. Stein, P. E., Boodhoo, A., Tyrrell, G. J., Brunton, J. L., and Read, R. J. (1992) *Nature 355*, 748−750.
6. Richardson, J. M., Evans, P. D., Homans, S. W., and DonohueRolfe, A. (1997) *Nat. Struct. Biol. 4*, 190−193.
7. Ling, H., Boodhoo, A., Hazes, B., Cummings, M. D., Armstrong, G. D., Brunton, J. L., and Read, R. J. (1998) *Biochemistry 37*, 1777−1788.
8. Nyholm, P. G., Brunton, J. L., and Lingwood, C. A. (1995) *Int. J. Biol. Macromol. 17*, 199−204.
9. Nyholm, P. G., Magnusson, G., Zheng, Z. Z., Norel, R., Binningtonboyd, B., and Lingwood, C. A. (1996) *Chem. Biol. 3*, 263−275.
10. Bax, A., Ikura, M., Kay, L. E., Torchia, D. A., and Tschudin, R. (1990) *J. Magn. Reson. 86*, 304−318.
11. Sklenár, V., Piotto, M., Leppik, R., and Saudek, V. (1993) *J. Magn. Reson. A 102*, 241−245.
12. London, R. E., Perlman, M. E., and Davis, D. G. (1992) *J. Magn. Reson. 97*, 79−98.
13. Tropp, J. (1980) *J. Chem. Phys. 72*, 6035−6044.
14. Asakura, T., Taoka, K., Demura, M., and Williamson, M. P. (1995) *J. Biomol. NMR. 6*, 227−236.
15. Williamson, M. P., and Asakura, T. (1993) *J. Magn. Reson. B 101*, 63−71.
16. Arepalli, S. R., Glaudemans, C. P. J., Daves, G. D., Kovac, P., and Bax, A. (1995) *J. Magn. Reson. B 106*, 195−198.
17. Fraser, R. R., Kaufman, M., Morand, P., and Govil, G. (1969) *Can. J. Chem. 47*, 403−409.
18. St. Hilaire, P. M., Boyd, M. K., and Toone, E. J. (1994) *Biochemistry 33*, 14452−14463.

BI980946+